

Semiconductor Nanocrystals-Reduced Graphene Composites for the Electrochemical Detection of Carbendazim

Paula C. A. Santana,^{a,b} Jéssica B. S. Lima,^{a,b} Tiago B. S. Santana,^b Luís F. S. Santos,^a
Charlene R. S. Matos,^a Luiz P. da Costa,^c Iara F. Gimenez^{ib a,d} and Eliana M. Sussuchi^{ib *a,b}

^aPrograma de Pós-Graduação em Química, Departamento de Química,
Universidade Federal de Sergipe, 49100-000 São Cristóvão-SE, Brazil

^bLaboratório de Corrosão e Nanotecnologia (LCNT),
Núcleo Regional de Competência em Petróleo, Gás e Biocombustíveis de Sergipe (NUPEG),
Universidade Federal de Sergipe, 49100-000 São Cristóvão-SE, Brazil

^cInstituto Tecnológico de Pesquisa de Sergipe (ITPS), 49020-380 Aracaju-SE, Brazil

^dPrograma de Pós-Graduação em Ciência e Engenharia de Materiais,
Universidade Federal de Sergipe, 49100-000 São Cristóvão-SE, Brazil

A new nanocomposite based on ZnCdTe semiconductor nanocrystals (NCs) synthesized *in situ* on reduced graphene oxide (rGO) was obtained. The heterostructure was characterized using UV-Vis emission and absorption spectroscopies, which provided evidences of the growth of the nanocrystals onto the rGO matrix. To evaluate the electrochemical performance, carbon paste electrodes modified with the nanocomposite (QD-rGO/CPE) were prepared, showing high sensitivity in the electroanalytical detection of the pesticide carbendazim. Under optimal operational conditions a calibration curve was constructed with a linear behavior in the range of 9.98×10^{-8} to 1.18×10^{-5} mol L⁻¹, with a correlation coefficient of 0.997. The limit of detection (LOD) and the limit of quantification (LOQ) for carbendazim were 9.16×10^{-8} and 2.78×10^{-7} mol L⁻¹, respectively. The electrode is successfully applied for the determination of carbendazim in orange juice samples.

Keywords: quantum dots, reduced graphene oxide, electrochemistry detection, carbendazim pesticide

Introduction

The nanocomposites used as modifiers of electrochemical sensors have been studied to increase the intensity of the responses/signals, improving performance in electroanalytical detections.¹ In this context, materials based on nanocrystals and graphene are promising due to the improvement of their properties with potential applications in electrochemical sensors² and photovoltaic devices,³ photocatalysis⁴ and photodetection.⁵ The nanocomposites can be obtained through the *in situ* growth of the semiconductor nanoparticles using graphene and its derivatives as matrix, providing an efficient electronic transport between nanomaterials with non-covalent intermolecular interactions.^{6,7} The stability of the nanocomposite based on nanoscale semiconductors and graphene can be improved by the strong interactions

between the constituent materials. Additionally, the receptor characteristics of the graphene dispersing the electrons in a conductive nanometric regime may promote an efficient separation of charges, making this material promising for electrochemical applications.^{8,9} In this context, the use of electrochemical methods using heterostructures is being explored not only as a characterization technique, but also in the development of analytical methodologies for detection of electroactive species.^{2,10} Matos *et al.*¹⁰ prepared electrodes modified with Cd_{1-x}Mg_xTe semiconductor nanocrystals and graphene-based materials. The simultaneous electrochemical determination of lidocaine and epinephrine showed high sensitivity and selectivity, using the differential pulse voltammetry technique for the detection of electroactive species.

Carbendazim (CBZ, methyl benzimidazol-2-ylcarbamate) is a pesticide widely used in Brazil to avoid and eliminate a variety of diseases in agricultural processes, especially in fruits. However, owing to its

*e-mail: esmidori@gmail.com

chemical stability, carbendazim is considered a persistent pollutant in soil and water. According to Brazilian Health Regulatory Agency (Anvisa), the risk of this pesticide is considered medium with toxicological classification III, a possible carcinogen in humans with maximum residue limit of $2.62 \times 10^{-5} \text{ mol L}^{-1}$ for citrus samples.¹¹

Many analytical techniques, including capillary electrophoresis, gas or liquid chromatography method, have been applied to develop effective methods for pesticides residue analysis.¹²⁻¹⁶ Chromatography techniques operate with high sensitivity and accuracy, but they suffer from complicated pretreatment steps using toxic organic solvent and also long analysis time, and most of them require expensive equipment. The use of electroanalytical methodologies has been an alternative in the detection of pesticides, since they are cheaper techniques with easier sample preparation and rapid analysis time, in addition to high sensitivity and selectivity.¹⁷⁻²¹

In this work, we described the preparation of reduced graphene/ZnCdTe semiconductor nanocrystal composites by growing the inorganic nanocrystals *in situ* onto the graphene sheets, and as well as a study of electrochemical determination of carbendazim pesticide in orange juice fruit by carbon paste electrodes modified with the reduced graphene/ZnCdTe composites.

Experimental

Materials

Tellurium powder (ca. 200 mesh, 99.8%), sodium borohydride (NaBH_4 , 98%), cadmium chloride hydrate ($\text{CdCl}_2 \cdot \text{H}_2\text{O}$, 98%), zinc chloride (ZnCl_2 , 99%), 3-mercaptopropionic acid (MPA, 99%), ascorbic acid (AA, $\text{C}_6\text{H}_8\text{O}_6$) were purchased from Sigma-Aldrich. Sodium hydroxide (NaOH) was purchased from Vetec. Graphite powder was purchased from Dinamica, potassium ferricyanide and ferrocyanide ($\text{K}_3(\text{Fe}(\text{CN})_6$ and $\text{K}_4(\text{Fe}(\text{CN})_6$) were purchased from J. T. Baker. For Britton-Robinson (BR) buffer solutions, we used orthophosphoric acid (H_3PO_4) from Synth. Acetic acid (H_3CCOOH) was purchased from Vetec. Boric acid (H_3BO_3) from Reagen, while analytical standard of carbendazim (purity > 98%) was pestanal (Sigma-Aldrich). Ultrapure water was in-laboratory produced from deionized water using an ultrapure water generator device, Millipore.

Preparation of graphene-based materials

The preparation of graphene-based materials using graphite as precursor was carried out by modified Hummers

method,^{10,22} followed by reduction with ascorbic acid to obtain reduced graphene oxide (rGO). This method was accomplished in two steps. First, 15.00 g of KMnO_4 were mixed to 5.00 g graphite in a 500 mL beaker, which was placed in an ice bath for the dropwise addition of 100 mL concentrated H_2SO_4 from a buret, under vigorous stirring. After this, a black sludge was formed, the beaker was removed from the ice bath and 400 mL water were added to the mixture. Then the resulting solution was heated at 90 °C for 1 h under constant stirring, when a dark yellow suspension was formed. The mixture was centrifuged, washed 3 consecutive times with water and the solid residue collected. In the second step, the reduction of the graphene oxide prepared in the first step was carried out by mixing 1.00 g graphene oxide with 10.00 g ascorbic acid in 50 mL deionized water, and kept under constant stirring at room temperature for 48 h to yield a yellow solution of reduced graphene oxide (rGO).

Preparation of ZnCdTe nanocrystals *in situ* onto reduced graphene oxide

In the methodology described for obtaining MPA-capped ZnCdTe nanocrystals onto rGO, initially 2 mL of the rGO solution was diluted to 40 mL (1 mg mL^{-1}) with ultrapure water. The resulting solution was used as the medium for dissolving the metallic precursors (CdCl_2 and ZnCl_2) and capping agent (MPA), adjusting pH to 9.0 with NaOH solution (0.2 mol L^{-1}), with 1:1:2 Zn: Cd: thiol stoichiometric proportions according to our previous report of $\text{Zn}_x\text{Cd}_{1-x}\text{Te}$ nanocrystals.²³ Separately, a NaHTe solution was freshly prepared in a Schlenk tube under N_2 atmosphere, by the addition of 0.064 g of Te powder and 1.50 g of NaBH_4 in 10 mL of water under vigorous stirring at 40 °C for 20 min, until the purple suspension became colorless. After the addition of NaHTe to the reaction medium containing the metallic precursors, the solution in the round bottomed flask became immediately orange and the mixture was transferred to a Teflon-lined stainless steel reactor for hydrothermal treatment at 100 °C for 70 min. After the hydrothermal treatment, the reaction medium was allowed to cool down to room temperature and the suspension was centrifuged at 4000 rpm and the collected precipitate was stored in a refrigerator. An analogous experiment was carried out using ultrapure water in the absence of rGO for the preparation of aqueous suspension of $\text{Zn}_x\text{Cd}_{1-x}\text{Te}$ nanocrystals.

Modified electrodes

Unmodified carbon paste electrodes containing 7:3 of graphite powder:mineral oil by weight were used for the

sake of comparison. The carbon paste modified electrodes containing ZnCdTe quantum dots and reduced graphene oxide (QD-rGO/CPE) were prepared by mixing graphite powder:QD-rGO:mineral oil (5:2:3 ratio). The carbon paste mixture holder was constructed using a thick-walled glass tube with 0.50 cm internal diameter. A copper sleeve equipped with a copper wire plunger was mounted at the top of the glass tube. By rotating the sleeve, the plunger extruded a used paste layer which was sliced off to form a fresh paste surface and was made by hand-polishing on a weighing paper. The electrodes used in the experiments were stored in a refrigerator at 4 °C and the measurements were performed at room temperature.

Analytical determination of carbendazim

A 0.01 mol L⁻¹ carbendazim stock solution was prepared using the solid dissolved in 5 mL of ultrapure water. The volumes suitable for electroanalytical procedure were taken from the stock solution and diluted to 10 mL in the electrochemical cell containing the supporting electrolyte. Carbendazim was determined with different carbon paste electrodes and analyzed by differential pulse voltammetry. All experiments were performed at room temperature.

Real samples consisting of orange fruits were purchased at a local street fair. The fruit juice was extracted with a manual extractor and, subsequently, the collected juice was centrifuged in two cycles of 4000 rpm for 10 min in order to remove residues.¹⁹ The samples were stored in an amber glass bottle in the refrigerator. An aliquot of the previously calculated volume of the carbendazim stock solution was diluted in methanol and added to the extracted juice for further analysis.

Characterization techniques

UV-Vis absorption spectroscopy measurements were performed using a PerkinElmer Lambda 45 spectrophotometer at room temperature in the 200-700 nm range. For the characterization of photoluminescence (PL) spectroscopy, a PerkinElmer LS 55 Luminescence Spectrometer was used, exciting samples at 350 nm. The electrochemical measurements were carried by using Autolab 100N Potentiostat/Galvanostat. Cyclic and differential pulse voltammetric experiments were performed in a one-compartment cell using a carbon paste working electrode, a platinum wire auxiliary electrode and Ag/AgCl/KCl (3.00 mol L⁻¹) reference electrode. The experiments were performed at 25 ± 1 °C and in borate buffer (pH 9.0). The solutions were deaerated with N₂ flow for 15 min and kept under this atmosphere during

the experiment. Transmission electron microscopy (TEM) images were obtained using a Jeol 2100 microscope operating at 200 kV. Samples were prepared by dropping isopropyl alcohol suspensions onto 400 mesh carbon-coated copper grids and allowing to dry under ambient atmosphere.

Results and Discussion

Description of ZnCdTe nanocrystals and graphene-based materials

The composite obtained from *in situ* growth ZnCdTe nanocrystals onto graphene-based materials was characterized by absorption and PL spectroscopy (Figure 1), as well as TEM measurements (Figure 2). Absorption and emission bands are assigned to electron transitions involving semiconductor valence and conduction bands. Both absorption and emission bands of rGO-supported ZnCdTe shifted to higher wavelengths compared to the aqueous colloidal ZnCdTe. This suggests that nanocrystal growth onto rGO sheets may favor the formation of larger particles due to nanocrystal aggregation, which is confirmed by TEM images (discussed below). PL spectra evidence also a decrease in the emission intensity for rGO-supported ZnCdTe, a behavior already reported for quantum dots grown onto graphene sheets¹⁰ related to nanocrystal to graphene charge transfer.

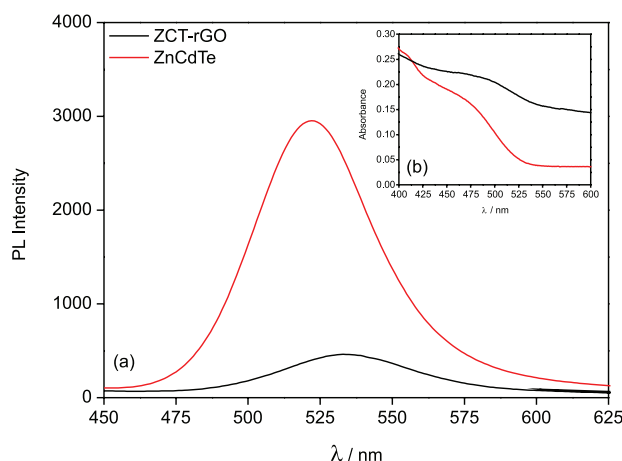


Figure 1. (a) Photoluminescence spectra (λ_{exc} 350 nm) for ZnCdTe and ZnCdTe-rGO samples; (b) UV-Vis absorption spectra for ZnCdTe and ZnCdTe-rGO samples.

TEM images (Figure 2) show that rGO sample obtained here has the typical sheet morphology with folded regions and transparent layers (Figure 2a). After ZnCdTe growth, the graphene sheets are coated by a large amount of nanocrystals, with some degree of aggregation (Figures 2b and 2c) and highly crystalline aspect, which is evidenced by

the presence of lattice fringes (Figure 2d). The observation of the lattice fringes allows to locate each individual nanocrystal and observe the nearly spherical shapes, with diameters below 10 nm.

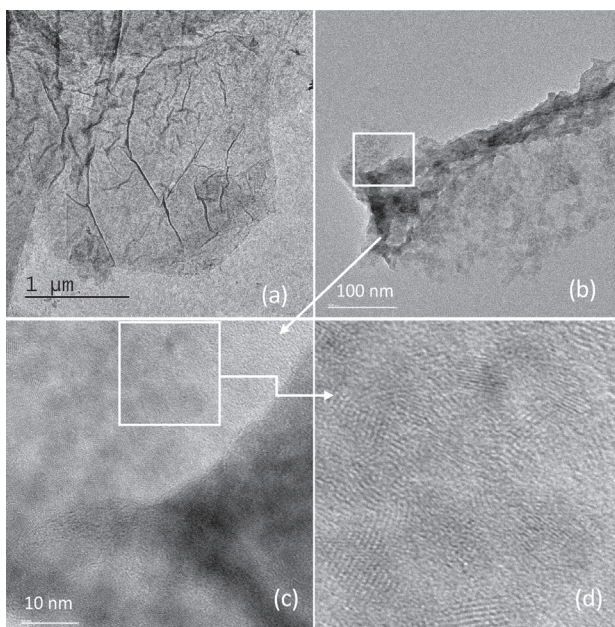


Figure 2. TEM images for rGO and ZnCdTe-rGO samples.

The electrochemical behavior of ZnCdTe nanocrystals grown in the presence of graphene was evaluated through the preparation of modified carbon paste electrodes. The Figure 3 shows cyclic voltammograms of the corresponding electrodes, showing that only the electrode modified with ZnCdTe/reduced graphene (rGO) exhibited anodic peak at +1.08 V and reduction peak at -1.25 V (*vs.* Ag/AgCl) in the potential range studied. According to a previous report by our research group,²³ ZnCdTe quantum dots obtained in aqueous medium showed an anodic peak related to oxidation of tellurium species in the core of nanocrystals^{24,25} and a reduction peak related to the reduction of the nanocrystals, forming a relatively stable radical anion (ZnCdTe^-).^{25,26} The separation between anodic and cathodic peaks was measured in order to estimate the value of electrochemical band gap ($\Delta E_{\text{elect}} = 2.33$ eV), which is in agreement to the optical band gap estimated from the PL band ($\Delta E_{\text{op}} = 2.32$ eV) and evidences the formation of the nanocrystals in the composite.

Optimization of electroanalytical parameters for pesticide determination

The influence of pH on the anodic differential pulse voltammograms of the QD-rGO/CPE was investigated using Britton-Robinson buffer over the pH 5.0-8.0 range.

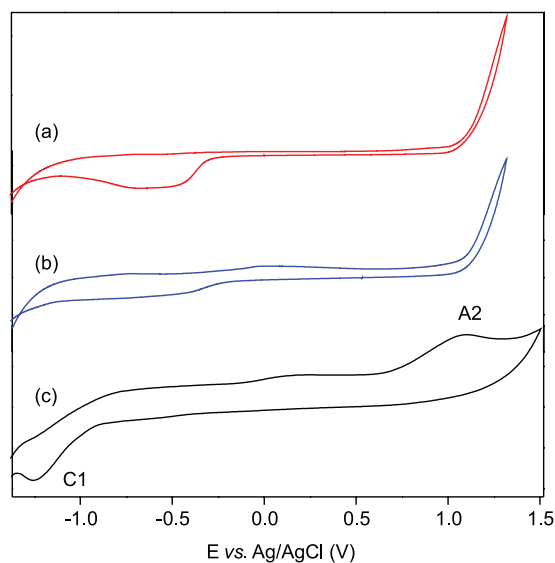


Figure 3. Cyclic voltammograms of carbon paste electrodes with different modifications: (a) bare; (b) rGO; (c) QD-rGO in borate buffered (pH = 9.0), scan rate 50 mV s⁻¹.

Figure 4 shows the presence of an intense and well defined oxidation peak in a slightly acidic condition (pH = 5.0). Considering that the pK_a value of carbendazim is 4.20, the net electrical charge in carbendazim molecule is pH-sensitive. Thus, under acidic conditions, that molecule is converted into its soluble salt, i.e., the deprotonated form, which favors the oxidation process. Figure S1 (Supplementary Information (SI) section) shows that a decrease of the analytical signal is observed at pH = 6.0, a phenomenon that can be attributed to the beginning of the degradation effect generating electroactive products that decrease the electroanalytical response. This behavior was also evidenced in the other pH values (7.0, 7.5, 8.0), due to the broadening of the anodic peak caused by the overlapping of carbendazim oxidation peaks with those of the electroactive species formed.^{27,28}

The electrode composition effect was studied by varying the amount of the composite in the graphite powder:mineral oil mixture. The anodic peak currents increased with increasing amount of QD-rGO composite up to 20% (m/m), for amounts higher than 20% the peak currents decreased significantly (Figure S2, SI section). Scan rate optimization evidenced that 20 mV s⁻¹ was a suitable choice due to the better analytical signal profile. The influence of the accumulation time on the oxidation response of carbendazim showed that the oxidation peak currents increased with extending accumulation time from 0 to 300 s. For longer times, a marked decrease in peak current was evidenced, indicating the saturation of the electrode surface.²⁴⁻²⁹ Therefore, the time of 300 s was selected in further experiments.

Electrochemical behaviors of the modified electrodes by determination of carbendazim pesticide

The performance of the modified carbon paste electrode (QD-rGO/CPE) towards the determination of carbendazim pesticide was studied by differential pulse voltammetry. Figure 4 shows the voltammogram characteristic of the bare carbon paste electrode (curve a), reduced graphene oxide (curve b) and QD-rGO (curve c) modified electrodes in presence of carbendazim under optimized conditions. The oxidation of carbendazim was evidenced by the presence of a well-defined peak at +0.88 V (Ag/AgCl) using QD-rGO/CPE, showing that the detection of carbendazim is enhanced by the presence of quantum dots and reduced graphene modification.

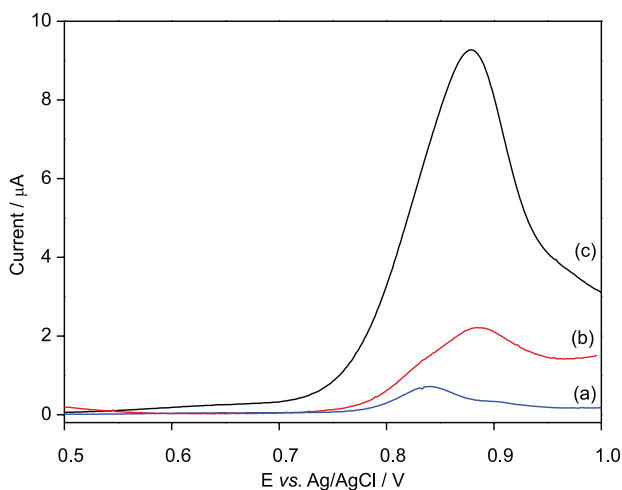


Figure 4. Differential pulse voltammograms of carbon paste electrodes with different modifications: (a) bare; (b) rGO; (c) QD-rGO in Britton-Robinson buffer solution (pH = 5.0) containing 5.0×10^{-5} mol L⁻¹ carbendazim, scan rate 20 mV s⁻¹.

Carbendazim was quantified using QD-rGO/CPE modified electrodes by differential pulse voltammetry (DPV). Figure 5 displays the voltammograms under optimized conditions for carbendazim measured with

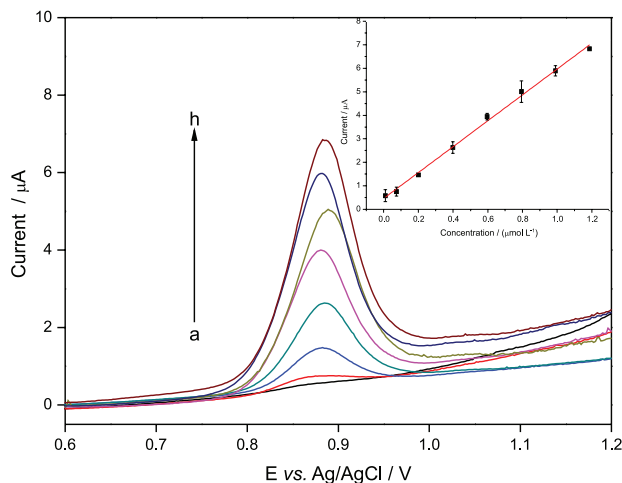


Figure 5. Differential pulse voltammograms measured with QD-rGO/CPE for different carbendazim concentrations (a-h): 0.01, 0.74, 2.00, 3.98, 5.96, 7.94, 9.90, 11.80 $\mu\text{mol L}^{-1}$ in Britton-Robinson (pH = 5.0), scan rate 20 mV s⁻¹ and analytical curve from the anodic peak currents (inset).

QD-rGO/CPE and the respective analytical curve (inset).

The observed anodic peak currents were proportional to the concentration of the corresponding carbendazim solutions (Figure 6). A linear relationship between the anodic peak currents and carbendazim concentration was observed from 9.98×10^{-8} to 1.18×10^{-5} mol L⁻¹, with linear fitting equation as $I_{pa} = 5.51[\text{CBZ}] + 4.62 \times 10^{-6}$, where I_{pa} is the anodic peak current and [CBZ] is concentration of carbendazim, with a linear correlation coefficient (R^2) of 0.997, detection limit (LOD) 9.16×10^{-8} mol L⁻¹ and quantification limit (LOQ) 2.78×10^{-7} mol L⁻¹. According to the report published by Anvisa,¹¹ the maximum residue limit allowed for carbendazim is 5.0 mg kg⁻¹ (2.62×10^{-5} mol L⁻¹). Therefore, the LOD and LOQ values of carbendazim using the modified electrode demonstrate that it is possible to detect this pesticide in real orange juice samples. Additionally, the results obtained here were comparable to other modified electrodes (Table 1). The increased sensitivity in the detection of CBZ using the

Table 1. Comparison analytical characteristics of some electrochemical sensors for carbendazim detection

Modified electrode	Technique	Limit of detection / (mol L ⁻¹)	Reference
GO-MWNTs/GCE	differential pulse voltammetry	5.0×10^{-9}	29
Amberlite-XAD2-GNS/GCPE	adsorptive stripping voltammetry	3.1×10^{-9}	18
Tricresyl phosphate/CPE	adsorptive stripping voltammetry	3.0×10^{-7}	30
SiO ₂ -MWCNT/GCE	square wave voltammetry	5.6×10^{-8}	20
Silicon OV-17/CPE	adsorptive stripping voltammetry	4.8×10^{-8}	31
QD-rGO/CPE	differential pulse voltammetry	9.2×10^{-8}	this work

GO-MWNTs/GCE: graphene oxide dispersed multi-walled carbon nanotubes composite modified glassy carbon electrode; Amberlite-XAD2-GNS/GCPE: graphene nanosheets and amberlite XAD-2 modified glassy carbon paste electrode; SiO₂-MWCNT/GCE: silica/multiwalled carbon nanotubes/glassy carbon electrode; Silicon OV-17/CPE: graphite electrode modified with silicone OV-17; QD-rGO/CPE: carbon paste modified electrodes with quantum dots and reduced graphene oxide.

electrode modified (QD-rGO/CPE) can be attributed to the synergistic effect of nanocrystals and reduced graphene oxide. The distribution of the ZnCdTe nanocrystals in the rGO sheet promotes an increase in the effective area of the electrode, increasing the amount of CBZ on the surface of the modified electrode. This effect and the conductivity of the hybrid material increase the electron transfer rate between electrode and the analyte facilitating the oxidation of the pesticide. The use of this electrode is also justified by the ease of preparation and regeneration of the electrode surface, allowing the rapid reading of the analyses in possible applications as a portable electrode.

An interference study of other electroactive species (ascorbic and citric acid, both commonly found in fruit juices) on the proposed method in the determination of carbendazim was also carried out. The selectivity of the QD-rGO/CPE was evaluated by DPV measurements in 5.0×10^{-5} mol L⁻¹ carbendazim solution with 0.1:1; 1:1; 10:1 of possible interfering species:CBZ ratios under the optimized conditions. The selectivity of the modified electrode for carbendazim detection in the presence of interfering species, showing only a slight increase of oxidation currents of carbendazim in the presence of interfering species. The repeatability of the method was evaluated in three different concentration ranges (5.96, 7.94 and 9.90 $\mu\text{mol L}^{-1}$) in triplicate. The results reveal that the electrode presented satisfactory repeatability, indicating the accuracy of the method with relative standard deviations of 3.7, 7.6 and 8.7%, respectively.

Real samples analysis

QD-rGO/CPE was used in the determination of CBZ in real orange juice samples. The experiments were performed by adding an aliquot of the 5% (v/v) sample to the supporting electrolyte in the presence of 10% MeOH to minimize matrix effects. Successive additions of the standard carbendazim solution were performed and the data show an increase in the anodic peak current proportional to the added analyte amount (Figure 6), according to the linear equation: $I_{pa}(A) = 1.51 \times 10^{-6} + 1.04[\text{CBZ}] (\text{mol L}^{-1})$, $R^2 = 0.993$. By linear extrapolation, the amount of carbendazim present in the sample was found to be

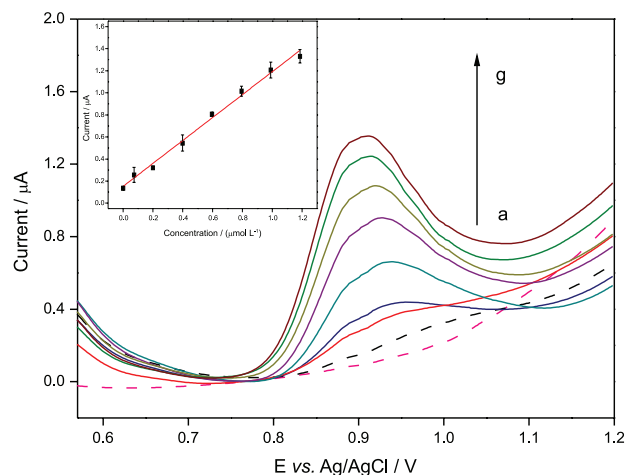


Figure 6. Differential pulse voltammograms do QD-rGO/CPE in absence of matrix (---, in red); in the presence of 5% orange juice (---, in black) and different concentrations of CBZ 0.74, 2.00, 3.98, 5.96, 7.94, 9.90, 11.80 $\mu\text{mol L}^{-1}$ (a-g) in Britton-Robinson (pH = 5.0), scan rate 20 mV s⁻¹. Inset: analytical curve from the anodic peak currents.

29.1 $\mu\text{mol L}^{-1}$ (5.56 ppm) in orange juice, indicating the presence of the pesticide in the sample. The recovery of the amounts of carbendazim added were calculated. The results obtained are shown in Table 2, with satisfactory recovery ranging from 93.3-99.7%, evidencing the viability in the proposed method.

Conclusions

The semiconductor nanocrystals obtained *in situ* onto the reduced graphene oxide matrix exhibited absorption and emission bands shifted to longer wavelengths compared to free nanocrystals, evidencing a synergic effect. The electrochemical characterization of the composite showed oxidation and reduction peaks typical of nanocrystals, demonstrating an efficient incorporation. The presence of semiconductor nanocrystals on the reduced graphene oxide facilitated an electron transfer between the electrode and solution, leading to an improved electrochemical response. An electrochemical method was developed for the determination of carbendazim, presenting LOD and LOQ values comparable to other sensors, which demonstrates the viability of its application for analyte detection. The proposed method was used in the analysis of

Table 2. Recovery study performed adding standard solutions of carbendazim diluted orange juice samples

[CBZ] electrochemistry cell / ($\mu\text{mol L}^{-1}$)	[CBZ] added / ($\mu\text{mol L}^{-1}$)	[CBZ] expected value / ($\mu\text{mol L}^{-1}$)	[CBZ] found / ($\mu\text{mol L}^{-1}$)	Recovery / %
1.46	0.74	2.20	2.19 ± 0.07	99.7
	5.96	7.42	7.27 ± 0.17	98.0
	9.90	11.36	10.60 ± 0.73	93.3

CBZ: carbendazim.

carbendazim residues in a real orange juice sample, leading to results above the values allowed by Anvisa (5 mg kg^{-1} , $2.62 \times 10^{-5} \text{ mol L}^{-1}$).

Supplementary Information

Supplementary data are available free of charge at <http://jbcs.sbq.org.br> as PDF file.

Acknowledgments

Authors are grateful to Brazilian funding agencies CNPq, CAPES and FAPITEC/SE for financial support, to LNLS for TEM measurements, to CLQM (Center of Chemistry Laboratories Multi-users) from Federal University of Sergipe for the analysis support and Prof Dr Sandro Navickiene for material support.

References

1. Marín, S.; Merkoçi, A.; *Electroanalysis* **2012**, *24*, 459.
2. Cincotto, F. H.; Moraes, F. C.; Machado, S. A. S.; *Chem. - Eur. J.* **2014**, *20*, 4746.
3. Guo, C. X.; Yang, H. B.; Sheng, Z. M.; Lu, Z. S.; Song, Q. L.; Li, C. M.; *Angew. Chem.* **2010**, *122*, 3078.
4. Xiang, Q.; Yu, J.; Jaroniec, M.; *Chem. Soc. Rev.* **2012**, *41*, 782.
5. Lu, Z.; Guo, C. X.; Yang, H. B.; Qiao, Y.; Li, C. M.; *J. Colloid Interface Sci.* **2011**, *353*, 588.
6. Katsukis, G.; Malig, J.; Schulz-drost, C.; Leubner, S.; Jux, N.; Guldi, D.; *ACS Nano* **2012**, *6*, 1915.
7. Chang, H.; Lv, X.; Zhang, H.; Li, J.; *Electrochemistry* **2010**, *12*, 483.
8. Cao, A.; Liu, Z.; Chu, S.; Wu, M.; Ye, Z.; Cai, Z.; Chang, Y.; Wang, S.; Gong, Q.; Liu, Y.; *Adv. Mater.* **2010**, *22*, 103.
9. Markad, G. B.; Battu, S.; Kapoor, S.; Haram, S. H.; *J. Phys. Chem.* **2013**, *117*, 20944.
10. Matos, C. R. S.; Souza Jr., H. O.; Santana, T. B. S.; Candido, L. P. M.; Cunha, F. G. C.; Sussuchi, E. M.; Gimenez, I. F.; *Microchim. Acta* **2017**, *184*, 1755.
11. <http://portal.anvisa.gov.br/programa-de-analise-de-registro-de-agrotoxicos-para>, accessed in February 2019.
12. Paranthaman, R.; Sudha, A.; Kumaravel, S.; *Am. J. Biochem. Biotechnol.* **2012**, *8*, 1.
13. Xiaowen, D.; Xianfeng, C.; Weijun, K.; Yinhu, Y.; Meihua, Y.; *RSC Adv.* **2015**, *5*, 86163.
14. Oskotskaya, E. R.; Gribanov, E. N.; Saunina, I. V.; *J. Anal.* **2017**, *72*, 206.
15. Boeris, V.; Arancibia, J. A.; Olivieri, A. C.; *Anal. Chim. Acta* **2014**, *814*, 23.
16. Kim, K.; Park, D.; Kang, G.; Kim, T.; Yang, Y.; Moon, S.; Choi, E.; Ha, D.; Kim, E.; Cho, B.; *Food Chem.* **2016**, *208*, 239.
17. Trojanowicz, M.; *Electroanalysis* **2002**, *14*, 19.
18. Khare, N. G.; Dar, R. A.; Srivastava, A. K.; *Electroanalysis* **2015**, *27*, 1915.
19. Petroni, J. M.; Lucca, B. G.; Fogliato, D. K.; Ferreira, V. S.; *Electroanalysis* **2016**, *28*, 1362.
20. Razzino, C. A.; Sgobbi, L. F.; Canevari, T. C.; Cancino, J.; Machado, S. A. S.; *Food Chem.* **2015**, *170*, 360.
21. Gou, Y.; Guo, S.; Li, J.; Wang, E.; Dong, S.; *Talanta* **2011**, *84*, 60.
22. Hummers Jr., W. S.; Offeman, R. E.; *J. Am. Chem. Soc.* **1958**, *80*, 1339.
23. Matos, C. R. S.; Candido, L. P. M.; Souza, H. O.; Costa, L. P.; Sussuchi, E. M.; Gimenez, I. F.; *Mater. Chem. Phys.* **2016**, *178*, 104.
24. Bae, Y.; Myung, N.; Bard, A. J.; *Nano Lett.* **2004**, *4*, 1153.
25. Poznyak, S. K.; Osipovich, N. P.; Shavel, A.; Talapin, D. V.; Gao, M.; Eychmuller, A.; Gaponik, N.; *J. Phys. Chem. B* **2005**, *109*, 1094.
26. Haram, S. K.; Quinn, B. M.; Bard, A. J.; *J. Am. Chem. Soc.* **2001**, *123*, 8860.
27. Li, Y.; Jiang, Y.; Mo, T.; Zhou, H.; Li, Y.; Li, S.; *J. Electroanal. Chem.* **2016**, *767*, 84.
28. Ya, Y.; Wang, T.; Xie, L.; Zhu, L.; Li, T.; Ning, D.; Yan, F.; *Anal. Methods* **2015**, *7*, 1493.
29. Luo, S.; Wu, Y.; Gou, H.; *Ionics* **2013**, *19*, 673.
30. Ashrafi, A. M.; Dordevic, J.; Guzsány, V.; Svancara, I.; Trtic-Petrovic, T.; Purenovic, M.; Vytras, K.; *Int. J. Electrochem. Sci.* **2012**, *7*, 9717.
31. Hernandez, P.; Ballesteros, Y.; Galan, F.; Hernandez, L.; *Electroanalysis* **1996**, *8*, 941.

Submitted: October 25, 2018

Published online: February 12, 2019

